A Phenological Comparison of NDVI Products within Contiguous United States

Jiaxun Chai

Thesis submitted to the faculty of the Virginia Polytechnic Institute and State University in partial fulfillment of the requirements for the degree of

MASTER OF SCIENCE
In
GEOGRAPHY

Kirsten M. de Beurs, Chair
James B. Campbell
Laurence W Carstensen

May 16th, 2011
Blacksburg, VA

Keywords: Phenology, NDVI, Eco-region, AVHRR, MODIS, SPOT

A Phenological Comparison of NDVI Products within Contiguous United States

Jiaxun Chai

ABSTRACT

This study computed the Normalized Difference Vegetation Index (NDVI) products derived from NOAA AVHRR, MODIS, and SPOT VGT sensors. NDVI products from different instruments vary in spatial resolution, temporal coverage and spectral range. As a result, multi-sensor NDVI products are rarely used in a single phenological study. In order to evaluate the difference and similarity of NDVI records from the three sensors, I used the EPA Eco-region framework to determine the average annual Start of Season (SOS) and End of Season (EOS) of Contiguous United States, and analyzed dates among datasets. In addition, I created 1127 sample points within the study area, and compared the relationship between SOS/EOS based on land cover. The objectives of this thesis are to: 1) compare multi-sensor NDVI data using phenological models, 2) define a strategy to merge multi-sensor NDVI products to a single phenological product without direct NDVI conversion. The spatial and statistical analysis revealed that the Land Surface Phenology (LSP) measurements retrieved from NDVI time series from different sensors follow linear and positive relationships where compared by either eco-region or sample point. The historical record of AVHRR combined with the modern MODIS and SPOT data provides a critical and reliable perspective on phenological patterns in Contiguous United States area. The success of this study will help LSP by providing understanding of how different instruments can be combined to generate multi-sensor NDVI data for phenology.

Acknowledgements

First of all, I would like to express my gratitude to my advisor Dr. Kirsten de Beurs, for her guidance and supports to my study and research. Although she moved to University of Oklahoma during my master program, I really appreciate her continuousness of being my supervisor. I can't imagine that any other advisor could provide online research discussion every Friday, respond to my every email in five minutes, and revise and edit my writing that patiently. Her commitment, enthusiasm, and accomplishment in remote sensing and phenology always inspire me to work hard in Phenology and convict my life to academia, if not now, in the near future. Without her, I might still being floundering outside the door of Phenology. I would also thank my co-advisor Dr. James Campbell, who helps me to improve my writing skills and broaden my horizons in the discipline of remote sensing. My sincere thanks also go to Dr. Laurence Carstensen, who offers me technical support of GIS program and teaches me most of what I know about geoprocessing.

I am also very grateful to others who have helped me through this program, especial Baojuan Zheng and Dong Yan, who give help for my research, and encourage me every time. Most importantly, I must thank my parents in China, and my aunt and her family in Florida. Their invaluable supports are the direction of my well-being since always.

Table of Contents

List of Figures

List of Tables

Chapter 1 Literature Review

1.1 Why Geography and Phenology?

Geography is a subject that makes people look at the world and make sense of it. Studying geography is not just to memorize the names and places.

" ..Mere names of places...are not geography...know by heart a whole gazetteer full of them would not, in itself, constitute anyone a geographer." -- William Hughes, 1863

Geographers are obligated to discover the spatial and temporal distribution of objects, phenomena and processes on the earth surface as well as the relationship between the environment and human being. Geography could be split into several sub-fields depending on disciplines.

Within physical geography, phenology is the science of studying life-cycle events of plants and animals, and their responses to seasonal and inter-annual variation in climate [*Morisette et al., 2008*]. Derived from the Greek, the word phenology means to show, to bring, to light, and make to appear, which indicates that this subject mainly focuses on the significant timing of biological events in their annual cycle. Land Surface Phenology (LSP) uses Remotely Sensed (RS) images to track the growth stages of green vegetation (emergence, growth, maturity, and harvest) at both local and global scale. More than five methods of observing LSP have been developed and widely used: 1) phenological observation networks; 2) phenological modeling; 3) eddy covariance flux towers; 4) global change experiments; and 5) using remotely sensed images [*White et al., 2009*].

Because the timing and events of plant life cycle were obtained from field data, early phenological studies deeply relied on plant observation networks [*Hopp, 1974*]. To further understand the relationship between biological events and environment, phenological models

were developed to examine how environmental factors such as (temperature, solar radiation, and climate) influence LSP [*Hunter and Lechowicz, 1992; Nienstaedt, 1974; Schwartz and Marotz, 1986*]. Information concerning the date of vegetation growth stage (such as the emergence of leaves and flowers, the fall in deciduous trees, and the date of leaf coloring) were considered as indicators to reveal the characteristics of the vegetative surface [*Schwartz and Karl, 1990*]. The use of these standardized indicators revealed the earlier arrival of spring in the Northern Hemisphere of the past few decades [*Chmielewski and Rötzer, 2001; Menzel et al., 2006*].

1.2 Remote Sensing

Remote sensing (RS) is a technique that uses a sensing device to collect information on given objects or phenomena from afar without physical contact. Hand held cameras, photographic instruments installed in aircrafts, and satellite sensors are devices that can be used in data gathering. RS technology allows us to collect large scale data of biological phenomenon from inaccessible regions [*Campbell, 2007*].

The success of phenology at large scale is attributed to the development of remote sensing technology [*Goward, 1989*]. *Moulin et al., (1997)* compared the traditional method of phenological research (using ground observation records) with new technology (capturing vegetative signals from RS images), and concluded that collecting data from RS technology is more efficient and effective than measuring data on the ground.

A summary of the satellite sensors that are frequently used in phenological analysis can be found in Table 1. The National Oceanic and Atmospheric Administration's (NOAA) Advanced Very High Resolution Radiometer (AVHRR) was launched in 1978. The primary application of AVHRR data is relevant to climate change and environmental degradation because it has a

record of 30 years of image collection, beginning in 1978 [*Badeck et al., 2004; Cramer et al., 2001*]. The NOAA sensor series provides twice daily images with global coverage, and five of them have carried AVHRR sensors (NOAA 7, 9, 11, 14, and 16). The Moderate Resolution Imaging Spectro-radiometers (MODIS) are carried by two platforms: the Terra and Aqua satellites, launched in 1999 and 2002, respectively. MODIS is a multi-spectral sensor. It has 36 bands with spatial resolution ranges from 250 to 1000 meters. The SPOT (Satellite Pour l'Observation de la Terre) satellite system was designed for exploring the earth's resources, climate, and human activities. VEGETATION 1 and VEGETATION 2 are two sensors installed on SPOT4 and SPOT5 satellites, which are operated by the VEGETATION programme. The SPOT4 and SPOT5 were launched in 1998 and 2002, respectively.

Although the increasing importance of using satellite remote sensing in phenological and ecological researches has been demonstrated [*Pettorelli et al., 2005*], constraints of RS images should also be addressed. RS technology offers an overview of the phenological condition of the earth surface in macro perspective; however, it doesn't capture the detailed phenophases of individual plants. Two major concerns of using remote sensed images in phenology are: 1) the lack of ground observation data for validation, and 2) inconsistency of image quality [*Badeck et al., 2004*]. Aside from ground observation, validation is sometimes conducted by comparing the results with images with finer temporal and spatial resolution [*de Beurs and Townsend, 2008*]. In order to improve the image quality, new approaches have been developed to filter noise and optimize the satellite signal.

1.3 Vegetation Index

Vegetation indices (VIs), which transform the spectral bands' signals of remote sensing instruments into digital information to represent the earth surface condition, enable the monitoring of dynamic variation of biophysical parameters [*Huete et al., 2002*]. The Normalized Difference Vegetation Index (NDVI) and the Enhanced Vegetation Index (EVI) data provide detailed insight into biotic activities [*Running et al., 1994*].

First introduced by *Tucker, (1979*), NDVI is commonly used to observe vegetation growth and dynamics [*Myneni et al., 1997*]. The performance of NDVI relies on the absorption of energy from red light by chlorophyll and scattering of near infrared energy by green plants. The decrease of red reflectance and increase of near-infrared make NDVI sensitive to canopy fluctuations. It can differentiate between vegetated and non-vegetated pixels within an image and assess whether the observed target contains living green vegetation or not. It is used to evaluate biotic activities on the earth's surface as well [*Lee et al., 2002*]. The NDVI is calculated from two bands reflectance of a sensor as follows:

NDVI= (NIR-RED) / (NIR+RED)

Where RED and NIR bands represent the spectral reflectance measurements in the red band and near infrared band, respectively

Theoretically, NDVI of a given pixel scales from -1 to +1. The observed NDVI range for a land surface with vegetation is from 0.05 to 0.8. A non-vegetated pixel typically has a value close to 0, and highly vegetative pixels have high positive values. NDVI saturates in high biomass regions such as the Amazon drainage area [*Huete et al., 2002*]. To overcome the problem of its rapid decrease of sensitivity at moderate to high green biomass [*Gitelson et al., 2003; Jenkins et al., 2002*], several authors have proposed a variety of alternative vegetation indices that are less sensitive to saturation. *Vina et al., (2004)* modified the NDVI into the Wide

Dynamic Range Vegetation Index (WDRVI), and tested its sensitivity within eco-regions across years. They found that a simple modification on standard AVHRR NDVI can enhance its sensitivity in area with moderate to high vegetation density. The Enhanced Vegetation Index (EVI) was first presented by *Huete et al., (1997)* as a substitute to NDVI in high vegetative areas. It is one of two global vegetation products (with NDVI) delivered in the MODIS vegetation data. EVI can be calculated as follows [*Huete et al., 1997*]:

$$\mathbf{EVI=2.5*(\rho_{NIR}-\rho_{Red}) / (1+ \rho_{NIR}+6* \rho_{Red}-7.5* \rho_{Blue})}$$

where ρ= atmospherically corrected surface reflectance, NIR = near infrared band, Red = red band, Blue = blue band

The disadvantage of EVI is the fact that it requires the incorporation of a blue reflectance band. While blue reflectance is available on newer satellites, EVI cannot be calculated for AVHRR data, because AVHRR sensor does not contain a blue reflectance band. To overcome this problem *Kim et al., (2007)* developed a new vegetation index called "EVI2", which is a two band combination of the Enhanced Vegetation Index (EVI) and NDVI. Equation of EVI2 as follows [*Jiang et al., 2008*]:

$$\mathbf{EVI2=2.5*(\rho_{NIR}-\rho_{Red}) / (1+ \rho_{NIR}+2.4* \rho_{Red})}$$

where ρ= atmospherically corrected surface reflectance, NIR = near infrared band, Red = red band

Similar to EVI, EVI2 does not have saturation problems in high biomass area. However, EVI2 is not as popular as NDVI products, which are available online as preprocessed products.

RS sensors with NIR and Red bands are able to provide information for NDVI images, such as AVHRR, MODIS, SPOT VGT, and Sea-viewing Wide Field-of-View Sensor (SeaWiFS). A

number of NDVI products are available to the public and free to download. The Global Inventory Modeling and Mapping Studies (GIMMS) group has collected more than 25 years of images and has developed them into NDVI products which are based on the records of AVHRR series sensors [*Tucker et al., 2005*]. Mainly used in change detection, deforestation, and land cover classification, AVHRR NDVI improves the detection of vegetation changes and extraction of canopy biophysical parameters at regional and global scale [*Goward et al., 1991*]. The Land Processes Distributed Active Archive Center (LP DAAC) provides MODIS NDVI images that are ready to use. SPOT VGT-S10/D10 NDVI products can be obtained from the *VEGETATION Programme*. It is believed that the SPOT-NDVI data improves the vegetation measurement spatially, spectrally, and radiometrically [*Tucker et al., 2005*].

1.4 Multi-sensor NDVI data

Available NDVI data differ in spatial resolution, spectral range, and temporal coverage (Table 1). For example, GIMMS AVHRR has about 30-years of NDVI data, while only about 10-years of data are available from modern and advanced sensors such as MODIS, SPOT and SeaWiFS. The spectral band width of the NIR and Red bands differ with each sensor, which results in differences of sensitivity to ground objects. Every instrument has its advantages and disadvantages; sensors were designed for various purposes. Although a 25-year data collection is still short for detecting or predicting vegetation growth [*White et al., 2009*], AVHRR-NDVI data provides a good overview of robust trends. However, AVHRR sensors were not designed for vegetation monitoring originally [*Teillet et al., 1997*]. The sensors are sensitive to water vapor in the atmosphere, which impacts the calculated NDVI value [*Cihlar et al., 2001*]. The data reduction method, which transfers the local area coverage AVHRR images to AVHRR-NDVI

data and changes spatial resolution from 1 km to 8 km, bears on its quality [*James and Kalluri, 1994*]. The orbital drift of the sensors during their lifetime influences the geometrical system and in turn affects the image quality [*Cihlar et al., 2001; Fensholt et al., 2009*]. Modern sensors like MODIS and SPOT have higher spatial resolution with improved capability of monitoring LSP [*Tucker et al., 2005*]. They are equipped with better navigation, atmospheric correction and improved radiometric sensitivity systems [*Gobron et al., 2000*]. The availability of modern global satellite sensor data meets the ever-increasing demand of LSP studies [*Justice et al., 2000*].

Many studies attempt to compare multi-source NDVI data with the aim of extending the available records for scientific measurements [*Kim et al., 2007; van Leeuwen et al., 2006*]. The objective of such researches is to optimize NDVI data collection with higher image quality and longer temporal coverage for future work. *Brown et al., (2006)* verified the possibility of merging the AVHRR records with that of the more modern sensors in order to provide a historical perspective on current vegetation activities.

1.5 Multi-sensor Data Comparison

Distinctive variation of spectral bands in Red and NIR makes multi-sensor NDVI data less directly comparable [*Teillet et al., 1997*]. Studies of direct comparison differ in methodologies. *Fensholt et al., (2009)* re-sampled NDVI images derived from AVHRR GIMMS, Terra MODIS, and SPOT VGT to the same resolution, performed linear least squares trends analysis on annual average NDVI of different datasets. The other experiments evaluated the relative and absolute differences of NDVI data within an area or several selected sites over the world [*Brown et al., 2006; Ramsey et al., 1995*].

Most studies chose the linear least squares regression trend analysis to determine the relationship between datasets. One research collected six years of surface reflection data (field measurement data) in Senegal and uses these data as explanatory variables in a regression analysis [*Fensholt et al., 2009*].

$NDVI_{Field} = 0.0012 * NDVI_{SPOT\ VGT} + 0.081;\ R^2 = 0.34$

$NDVI_{Field} = 0.0007 * NDVI_{MODIS\ Terra} + 0.096;\ R^2 = 0.61$

$NDVI_{Field} = -0.0009 * NDVI_{AVHRR\ GIMMS} + 0.090;\ R^2 = 0.90$

where the annual average Terra MODIS, SPOT VGT and AVHRR GIMMS NDVI data are used as independent variables, field observed NDVI is the dependent variable.

Data used as independent variables were: AVHRR-NDVI 15 day's composite, MODIS-NDVI 16 day's composite, and SPOT-NDVI 10 day's composite. *Brown et al., (2006)* carried out pair-wise comparisons for NDVI images from AVHRR, SPOT, SeaWiFS, Landsat, and MODIS sensors. They did not collect ground data; instead, historical dataset AVHRR-NDVI was set as dependent variable in their analysis. EVI2 was used as reference index in a comparison carried out by *Kim et al., (2007)* in the Brazilian rain forest. The expected result was that EVI2 could perform as a substitute Vegetation Index for NDVI and EVI in cross sensor application.

Fensholt et al., (2009) revealed a good agreement between AVHRR and MODIS datasets, which was reflected by a high R-Square value of the regression lines. They concluded that AVHRR and MODIS data have closer similarity than the other sensor combinations. The difference and similarity between datasets were discussed by *Brown et al., (2006)* as well. By showing Root Mean Square Error (RMSE) and R-square, considerable similarities between AVHRR, MODIS, SPOT, and SeaWiFS for all 22 study sites were found, except one. Evidences of the resemblance among NDVI sources verified the possibility of long term vegetation monitoring and prediction studies by using integrated multi-sensor NDVI data.

The difference in spatial resolution increases the difficulty of multi-sensor NDVI comparison. A common method is to solve this problem is to standardize the spatial resolution of multiple datasets. For example, *Brown et al., (2006)* aggregated all datasets to one degree before comparison. Unfortunately, dataset combination responded to the resample process differently *Fensholt et al., (2009).* As mentioned above, the vegetative sensitivity of AVHRR-NDVI changes as the spatial resolution downgrades [*James and Kalluri, 1994*].

1.6 Geographic Frameworks

The NDVI data responds differently to surface vegetation consistent with the variation of geographic locations. In *Brown et al., (2006)*'s comparison work; multi-sensor datasets have higher agreement in southern latitudes. A possible reason is that the northern regions have longer periods of snow/ice cover than the southern regions, and areas with mixed vegetation and snow/ice cover generate more noisy pixels than other images [*Riggs and Hall, 2004*]. As a result, selection of geographic framework is significant to data comparison. Previous NDVI comparisons differ in selection of geographic framework [*Ramsey et al., 1995; Fensholt et al., 2009; Kim et al., 2007*]. Some works assessed data at regional scale, such as a state or a drainage area [*Ramsey et al., 1995; Kim et al., 2007*]; while *Brown et al., (2006)* carried out their analysis at global scale. They selected windows of 25 * 25 km and one degree centered on the 13 Earth Observation System Land Validation core sites.

Many agencies developed geographic frameworks for North America based on ecological, environmental, and geological characteristics. The US Environmental Protection Agency (EPA) eco-region systems level I and level II divide North America into 15 and 50 categories, respectively. The level III eco-region system further separated North America into 182 sub-

categories [*Omernik, 1995; 2004*]. Originally shown on the 1976 map "Eco-regions of the United States", a new eco-region system of the United States was developed by the US Forest Service in 1980 [*Bailey, 1983*]. There are 34 eco-regions that cover the Contiguous US plus 15 regions in Alaska and 2 in Hawaii. Another geographic framework is the pheno-region system [*White et al., 1997*], which identifies 500 pheno-regions across the globe using the AVHRR global 8- km NDVI data (8km, from 1982 to 1999) and monthly global climatology data from 1961 to 2009. The initial purpose of the division was to identify the phenological systems of the world for long-term biospherical study.

The eco-region system displays the regional patterns that are related to climate, soils, vegetation, and physiography [*Omernik, 1987*]. Spectral signal captured by remote sensing instruments reflect the biotic and abiotic features of earth surface, and express a similar context defined by Omernik's eco-region map. Eco-regions help to characterize the variation of vegetation components within different areas [*Ramsey et al., 1995*]. It can be used as geographic reference in phenology [*Thenkabail, 2004; Vina et al., 2004*].

1.7 Image Quality

Variation in image quality of NDVI data is caused by differences in sensor bandwidth and atmospheric conditions. The near-infrared band of AVHRR sensor overlaps the wave length where a great amount of the observed signal is absorbed by water vapor in the atmosphere, alternating the NDVI [*Cihlar et al., 2001; Holben, 1986*]. Atmospheric correction reduces atmospheric effects, and improves image accuracy and quality [*Joseph, 1995*]. To overcome the distraction made by clouds, *Brown et al., (2006)* stretched the time series to 16-day composites by the maximum value compositing (MVC). The MVC technology selects the pixels with

maximum value from a series of single composite images [*Holben, 1986*]. It eliminates the atmospheric effects of data collection by minimizing the cloud contamination, shadow effects, and aerosol and water-vapor effects [*Cihlar et al., 1994*]. Although MVC enables to optimize image with less atmospheric influence, it is limited if using images with short compositing periods [*Saleous et al., 2000*].

Variability of data quality is generated by product providers as well. Impacts from Bidirectional Reflectance Distribution Function (BRDF), and difference of the Spectral Response Functions used in products can lead to the difference in NDVI data [*Roujean et al., 1992; Trishchenko et al., 2002*]. Uncertainties from water vapor, ozone and aerosol (AOT) affect the reliability of products without atmospheric correction. *Nagol et al., (2009)* found that the AVHRR-NDVI products (data without any atmospheric correction) have lower quality than Pathfinder AVHRR Land (PAL) or LTDR data (a product that has been corrected for the Rayleigh scattering and ozone).

1.8 Phenological Methods

The Start of Season and End of Season (SOS/EOS) can be defined as rapid sustained increase/decrease in remotely sensed greenness after/before the longest annual period of photosynthetic senescence [*White et al., 2009*]. In reality, these measures are thought to represent the process or rapid events like green-up, leaf-out, and leaf-loss. Phonological characteristics are typically calculated by pixel. As a result, it is difficult to select an appropriate method to determine the Start of Season/End of Season (SOS/EOS) of a region by RS image without ground observation. *de Beurs and Henebry, (2010)* divided 12 different methods to determine

SOS by using RS images into four categories: thresholds, derivatives, smoothing functions, and fitted models.

Setting an arbitrary threshold is the simplest way to determine the SOS/EOS in RS images [*Fischer, 1994; Lloyd, 1990; Zhou et al., 2003*]. Usually the SOS is determined when the annual NDVI curve first arrives at certain value; while EOS is determined as the day of the year when threshold is reached again in downward direction of the curve. In the northern hemisphere, pixels in the South generate earlier SOS dates than pixels in the North and threshold of SOS determination varies. Setting a unique threshold value cannot satisfy the phenological pattern of area in continental scale. Many attempts have been made to understand different SOS methods and their fitness to ground data [*Schwartz et al., 2002; White et al., 2009*]. *White et al., (2009)* explored the difference of ten SOS/EOS estimation methods that used in recent phenological researches. A case study with the extent of North America was presented to discuss those 10 methods. After running those estimation models, they identified two as the most consistent models: Harmonic Analyses of NDVI Time Series - Fast Fourier Transform (HANTS-FFT), and Midpoint $_{pixel}$.

White et al., (1997) developed a formula to transform NDVI value (ranges from -1 to 1) to NDVI $_{ratio}$ as follows,

$$\mathbf{NDVI_{ratio} = (NDVI - NDVI_{min}) / (NDVI_{max} - NDVI_{min})}$$

where NDVI is the daily NDVI value, NDVI $_{max}$ is the annual maximum NDVI, and NDVI $_{min}$ is the annual minimum NDVI. Midpoint $_{pixel}$ is defined as NDVI $_{ratio}$ = 50%. Application of this equation may differ in defining the maximum and minimum NDVI value. For example, *White et al., (1997)* identified NDVI $_{max}$ - NDVI $_{min}$ as the range of annual NDVI flux, while *Kogan, (1995)* defined these two parameters as maximized and minimized NDVI in long term.

1.9 Problem Statement

NDVI products from different instruments vary in spatial resolution, temporal coverage and spectral range. In recent phenological studies, multi-sensor NDVI products are rarely used due to insufficient knowledge of difference and similarity between multiple data. Previous work verified the possibility of translating NDVI data from historical AVHRR sensor to modern and advanced ones [*Brown et al., 2006*]. Based on a review of former studies, I propose my research question: if compared within a geographic framework, like eco-regions, what is the relationship between SOS/EOS results estimated by multi-sensor NDVI data? Future phenological research can use multi-sensor NDVI data without concern of data conversion, if a linear relationship between SOS/EOS estimation is verified. I am filling the gap by using alternative method for data comparison. To avoid geometric errors, eco-regions are chosen as the unit for comparison. In addition, I have selected random sample points over different land cover categories within the study area. A phenological comparison will be carried out based on eco-region and land cover.

Reference List

Badeck, F. W., A. Bondeau, K. Böttcher, D. Doktor, W. Lucht, J. Schaber, and S. Sitch (2004), Responses of spring phenology to climate change, *New Phytologist*, *162*(2), 295-309.

Bailey, R. (1983), Delineation of ecosystem regions, *Environmental Management*, *7*(4), 365-373.

Brown, M., J. Pinzón, K. Didan, J. Morisette, and C. Tucker (2006), Evaluation of the consistency of long-term NDVI time series derived from AVHRR, SPOT-vegetation, SeaWiFS, MODIS, and Landsat ETM+ sensors, *Geoscience and Remote Sensing, IEEE Transactions on*, *44*(7), 1787-1793.

Campbell, J. B. (2007), *Introduction to remote sensing*, The Guilford Press.

Chmielewski, F. M., and T. Rötzer (2001), Response of tree phenology to climate change across Europe, *Agricultural and Forest Meteorology*, *108*(2), 101-112.

Cihlar, J., D. Manak, and M. D'iorio (1994), Evaluation of compositing algorithms for AVHRR data over land, *Geoscience and Remote Sensing, IEEE Transactions on*, *32*(2), 427-437.

Cihlar, J., I. Tcherednichenko, R. Latifovic, Z. Li, and J. Chen (2001), Impact of variable atmospheric water vapor content on AVHRR data corrections over land, *Geoscience and Remote Sensing, IEEE Transactions on*, *39*(1), 173-180.

Cramer, W., A. Bondeau, F. I. Woodward, I. C. Prentice, R. A. Betts, V. Brovkin, P. M. Cox, V. Fisher, J. A. Foley, and A. D. Friend (2001), Global response of terrestrial ecosystem structure and function to CO2 and climate change: results from six dynamic global vegetation models, *Global Change Biology*, *7*(4), 357-373.

de Beurs, K., and P. Townsend (2008), Estimating the effect of gypsy moth defoliation using MODIS, *Remote Sensing of Environment*, *112*(10), 3983-3990.

de Beurs, K., and G. M. Henebry (2010), Spatio-temporal statistical methods for modelling land surface phenology, *Phenological Research*, 177-208.

de Beurs, K., C. Wright, and G. Henebry (2009), Dual scale trend analysis for evaluating climatic and anthropogenic effects on the vegetated land surface in Russia and Kazakhstan, *Environmental Research Letters*, *4*, 045012.

Ramsey, R. Douglas, A. Falconer, and J. Jensen (1995), The relationship between NOAA-AVHRR NDVI and ecoregions in Utah, *Remote Sensing of Environment*, *53*(3), 188-198.

Fensholt, R., K. Rasmussen, T. Nielsen, and C. Mbow (2009), Evaluation of earth observation based long term vegetation trends--Intercomparing NDVI time series trend analysis consistency of Sahel from AVHRR GIMMS, Terra MODIS and SPOT VGT data, *Remote Sensing of Environment*, *113*(9), 1886-1898.

Fischer, A. (1994), A model for the seasonal variations of vegetation indices in coarse resolution data and its inversion to extract crop parameters, *Remote Sensing of Environment*, *48*(2), 220-230.

Gitelson, A. A., A. Viña, T. J. Arkebauer, D. C. Rundquist, G. P. Keydan, and B. Leavitt (2003), Remote estimation of leaf area index and green leaf biomass in maize canopies.

Gobron, N., B. Pinty, M. Verstraete, and J. Widlowski (2000), Development of spectral indices optimized for the VEGETATION Instrument.

Goward, S. N. (1989), Satellite Bioclimatology, *Journal of Climate*, *2*, 710-720.

Goward, S. N., B. Markham, D. G. Dye, W. Dulaney, and J. Yang (1991), Normalized difference vegetation index measurements from the Advanced Very High Resolution Radiometer, *Remote Sensing of Environment*, *35*(2-3), 257-277.

Holben, B. (1986), Characteristics of maximum-value composite images from temporal AVHRR data, *International Journal of Remote Sensing*, *7*(11), 1417-1434.

Hopp, R. J. (1974), Plant phenology observation networks, edited, pp. 25–43, Springer.

Huete, A., H. Liu, K. Batchily, and W. Van Leeuwen (1997), A comparison of vegetation indices over a global set of TM images for EOS-MODIS, *Remote Sensing of Environment*, *59*(3), 440-451.

Huete, A., K. Didan, T. Miura, E. P. Rodriguez, X. Gao, and L. G. Ferreira (2002), Overview of the radiometric and biophysical performance of the MODIS vegetation indices, *Remote Sensing of Environment*, *83*(1-2), 195-213.

Hunter, A. F., and M. J. Lechowicz (1992), Predicting the timing of budburst in temperate trees, *Journal of Applied Ecology*, *29*(3), 597-604.

James, M., and S. N. V. Kalluri (1994), The Pathfinder AVHRR land data set: an improved coarse resolution data set for terrestrial monitoring, *International Journal of Remote Sensing*, *15*(17), 3347-3363.

Jenkins, J., B. Braswell, S. Frolking, and J. Aber (2002), Detecting and predicting spatial and interannual patterns of temperate forest springtime phenology in the eastern US, *Geophys. Res. Lett*, *29*(24), 2201.

Jiang, Z., A. R. Huete, K. Didan, and T. Miura (2008), Development of a two-band enhanced vegetation index without a blue band, *Remote Sensing of Environment*, *112*(10), 3833-3845.

Joseph, H. (1995), Efficient Algorithms for Atmospheric Correction of Remotely Sensed Data, Citeseer.

Justice, C., A. Belward, J. Morisette, P. Lewis, J. Privette, and F. Baret (2000), Developments in the'validation'of satellite sensor products for the study of the land surface, *International Journal of Remote Sensing*, *21*(17), 3383-3390.

Kim, Y., A. R. Huete, Z. Jiang, and T. Miura (2007), Multisensor reflectance and vegetation index comparisons of Amazon tropical forest phenology with hyperspectral Hyperion data, *Remote Sensing and Modeling of Ecosystems for Sustainability IV*, *6679*(667906-1).

Kogan, F. N. (1995), Droughts of the late 1980s in the United States as derived from NOAA polar-orbiting satellite data, *Bulletin of the American Meteorological Society*, *76*(5), 655-668.

Lee, R., F. Yu, K. Price, J. Ellis, and P. Shi (2002), Evaluating vegetation phenological patterns in Inner Mongolia using NDVI time-series analysis, *International Journal of Remote Sensing*, *23*(12), 2505-2512.

Lloyd, D. (1990), A phenological classification of terrestrial vegetation cover using shortwave vegetation index imagery, *International Journal of Remote Sensing*, *11*(12), 2269-2279.

Menzel, A., T. H. Sparks, N. Estrella, E. Koch, A. Aasa, R. Ahas, K. ALM KÜBLER, P. Bissolli, O. G. BraslavskÁ, and A. Briede (2006), European phenological response to climate change matches the warming pattern, *Global Change Biology*, *12*(10), 1969-1976.

Morisette, J., A. Richardson, A. Knapp, J. Fisher, E. Graham, J. Abatzoglou, B. Wilson, D. Breshears, G. Henebry, and J. Hanes (2008), Tracking the rhythm of the seasons in the face of global change: phenological research in the 21st century.

Moulin, S., L. Kergoat, N. Viovy, and G. Dedieu (1997), Global-scale assessment of vegetation phenology using NOAA/AVHRR satellite measurements, *Journal of Climate*, *10*(6), 1154-1170.

Myneni, R. B., C. Keeling, C. Tucker, G. Asrar, and R. Nemani (1997), Increased plant growth in the northern high latitudes from 1981 to 1991, *Nature*, *386*(6626), 698-702.

Nagol, J. R., E. F. Vermote, and S. D. Prince (2009), Effects of atmospheric variation on AVHRR NDVI data, *Remote Sensing of Environment*, *113*(2), 392-397.

Nienstaedt, H. (1974), Genetic variation in some phenological characteristics of forest trees, *Phenology and Seasonality Modelling*, *Springer-Verlag, New York*, 389-400.

Omernik, J. (1987), Ecoregions of the conterminous United States, *Annals of the Association of American geographers*, *77*(1), 118-125.

Omernik, J. (1995), Ecoregions: a spatial framework for environmental management, *Biological assessment and criteria: tools for water resource planning and decision making*, 49–62.

Omernik, J. (2004), Perspectives on the nature and definition of ecological regions, *Environmental Management*, *34*, 27-38.

Pettorelli, N., J. Vik, A. Mysterud, J. Gaillard, C. Tucker, and N. Stenseth (2005), Using the satellite-derived NDVI to assess ecological responses to environmental change, *Trends in Ecology & Evolution*, *20*(9), 503-510.

Riggs, G., and D. Hall (2004), Snow mapping with the MODIS Aqua instrument.

Roujean, J., M. Leroy, A. Podaire, and P. Deschamps (1992), Evidence of surface reflectance bidirectional effects from a NOAA/AVHRR multi-temporal data set, *International Journal of Remote Sensing*, *13*(4), 685-698.

Running, S., C. Justice, V. Salomonson, D. Hall, J. Barker, Y. Kaufmann, A. Strahler, A. Huete, J. P. Muller, and V. Vanderbilt (1994), Terrestrial remote sensing science and algorithms planned for EOS/MODIS, *International Journal of Remote Sensing*, *15*(17), 3587-3620.

Saleous, N. Z. E., E. Vermote, C. Justice, J. Townshend, C. Tucker, and S. Goward (2000), Improvements in the global biospheric record from the Advanced Very High Resolution Radiometer (AVHRR), *International Journal of Remote Sensing*, *21*(6), 1251-1277.

Schwartz, M. D., and G. A. Marotz (1986), An approach to examining regional atmosphere-plant interactions with phenological data, *Journal of biogeography*, *13*(6), 551-560.

Schwartz, M. D., and T. R. Karl (1990), Spring phenology: nature's experiment to detect the effect of Green-up on surface maximum temperatures, *Monthly weather review*, *118*(4), 883-890.

Schwartz, M. D., B. Reed, and M. A. White (2002), Assessing satellitederived start-of-season (SOS) measures in the conterminous USA, *International Journal of Climatology*, *22*(14), 1793-1805.

Teillet, P., K. Staenz, and D. William (1997), Effects of spectral, spatial, and radiometric characteristics on remote sensing vegetation indices of forested regions, *Remote Sensing of Environment*, *61*(1), 139-149.

Thenkabail, P. (2004), Inter-sensor relationships between IKONOS and Landsat-7 ETM+ NDVI data in three ecoregions of Africa, *International Journal of Remote Sensing*, *25*(2), 389-408.

Trishchenko, A. P., J. Cihlar, and Z. Li (2002), Effects of spectral response function on surface reflectance and NDVI measured with moderate resolution satellite sensors, *Remote Sensing of Environment*, *81*(1), 1-18.

Tucker, C. (1979), Red and photographic infrared linear combinations for monitoring vegetation, *Remote Sensing of Environment*, *8*(2), 127-150.

Tucker, C., J. Pinzón, M. Brown, D. Slayback, E. Pak, R. Mahoney, E. Vermote, and N. El Saleous (2005), An extended AVHRR 8-km NDVI dataset compatible with MODIS and SPOT vegetation NDVI data, *International Journal of Remote Sensing*, *26*(20), 4485-4498.

van Leeuwen, W., B. Orr, S. Marsh, and S. Herrmann (2006), Multi-sensor NDVI data continuity: Uncertainties and implications for vegetation monitoring applications, *Remote sensing of environment*, *100*(1), 67-81.

Vina, A., A. A. Gitelson, D. C. Rundquist, G. P. Keydan, B. Leavitt, and J. Schepers (2004), Monitoring Maize. Phenology with Remote Sensing.

White, M., P. Thornton, and S. Running (1997), A continental phenology model for monitoring vegetation responses to interannual climatic variability, *Global Biogeochemical Cycles*, *11*(2), 217-234.

White, M., K. de Beurs, K. Didan, D. Inouye, A. Richardson, O. Jensen, J. O'Keefe, G. Zhang, R. Nemani, and W. van Leeuwen (2009), Intercomparison, interpretation, and assessment of spring phenology in North America estimated from remote sensing for 1982–2006, *Global Change Biology*, *15*(10), 2335-2359.

Zhou, L., R. Kaufmann, Y. Tian, R. Myneni, and C. Tucker (2003), Relation between interannual variations in satellite measures of northern forest greenness and climate between 1982 and 1999, *J. Geophys. Res*, *108*, 4004.

Definition

Land Surface Phenology (LSP): is the study of the spatio-temporal patterns in the vegetated land surface as observed by synoptic sensors at spatial resolutions and extents relevant to boundary layer processes.

Phenophase: an observable stage or phase in the annual life cycle of a plant or animal that can be defined by a start and end point. Phenophases generally have duration of a few days or weeks.

Remote Sensing (RS): is the science of acquiring and analyzing information about objects or phenomena from a distance.

NDVI: Normalized Difference Vegetation Index

EVI: Enhanced Vegetation Index

Eco-region: is an ecologically and geographically defined area that is smaller than an eco-zone and larger than an ecosystem

AVHRR: Advanced Very High Resolution Radiometer

MODIS: The Moderate Resolution Imaging Spectro-radiometer

SPOT: Satellite Pour l'Observation de la Terre

SOS/EOS: Start of Season/ End of Season

Tables and Figures

Table 1 Attributes of Available NDVI Products

Sensor	AVHRR	SPOT VGT	MODIS
Satellites	NOAA-7, 9, 11, 14, and 16	SPOT4 and SPOT 5	Terra and Aqua
Launched Date	23 Jun 1981 (NOAA-7)	24 Mar 1998 (SPOT4)	18 Dec 1999 (Terra)
Data Source	GIMMS NDVI	VEGETATION Programme	LP DAAC
Red/NIR Band (μm)	(0.5-0.7)/(0.7-1.1)	(0.61-0.68)/(0.78-0.89)	(0.62-0.67)/(0.84-0.87)
Spatial Resolution(km)	8	1	5.6
Temporal Resolution (day)	15	10	16
Coverage	Global	North America	Global

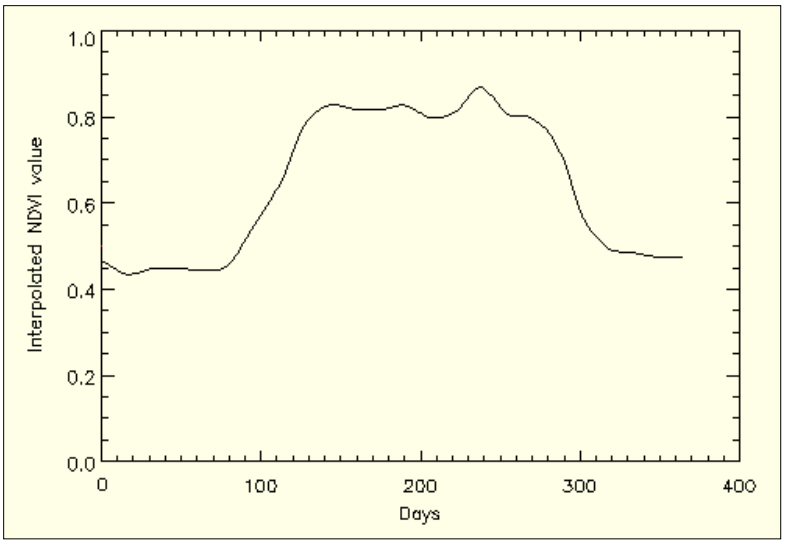

Figure 1 Annual Curve of MODIS NDVI in 2005

(Blacksburg, Virginia)

Chapter 2
A Phenological Comparison of NDVI Products within Contiguous United States

Jiaxun Chai

Department of Geography, Virginia Tech, Blacksburg, Virginia

Abstract

This study used the Normalized Difference Vegetation Index (NDVI) products derived from NOAA AVHRR, MODIS, and SPOT VGT sensors. NDVI products from different instruments vary in spatial resolution, temporal coverage and spectral range. As a result, multi-sensor NDVI products are rarely used in a single phenological study. In order to evaluate the difference and similarity of NDVI records from the three sensors, I used EPA Eco-region frameworks to determine the average annual Start of Season (SOS) and End of Season (EOS) of Contiguous United States, and analyzed dates among datasets. In addition, I created 1127 sample points within the study area, and compared the relationship between SOS/EOS based on land cover. The objectives of this thesis are to 1) compare multi-sensor NDVI data using phenological models, 2) define a strategy to merge multi-sensor NDVI products to a single phenological product without direct NDVI conversion. The spatial and statistical analysis revealed that the Land Surface Phenology (LSP) measurements retrieved from NDVI time series from different sensors follow linear and positive relationships where compared by either eco-region or sample point. The historical record of AVHRR combined with the modern MODIS and SPOT data provides a critical and reliable perspective on phenological patterns in Contiguous United States area.

Index Terms: Phenology, NDVI, Eco-region, AVHRR, MODIS, SPOT

2.1 Introduction

Phenology is the science of studying life-cycle events [*Morisette et al., 2008*]. Land Surface Phenology (LSP) uses Remote Sensing (RS) images to track green vegetation growth stages (emergence, growth, maturity, and harvest) both locally and globally. LSP plays a significant role in understanding the timing of current phenological shifts and their effects on plants and animals [*Heumann et al., 2007*].

Two methods are mainly used to monitor phenology of a region, 1) by field observation and 2) through RS analysis. Due to the spatial and temporal constrains of field phenological studies, remote sensing provides more efficient means for monitoring regional or global-scale phenological studies [*Moulin et al., 1997; Reed et al., 1994; Zhang et al., 2003*]. Rather than observing the specific phenological events like emergence of leave, flowering, and fruiting, remote sensing images enable the large scale determination of defined phenophases like Start of Season/End of Season (SOS/EOS), length of growing season, and peak photosynthetic activity [*Heumann et al., 2007*]. Vegetation indices (VIs) such as leaf area index (LAI) and fraction of absorbed photosynthetic active radiation (FAPAR) are widely used to observe and predict these vegetative phenophases on the earth's surface [*Kang et al., 2003; Myneni et al., 2002*]. The Normalized Difference Vegetation Index (NDVI), first introduced in Remote Sensing by Tucker, (1979), is one of the most frequently used Vegetation Indices in LSP. NDVI is defined as the difference between the near infrared (NIR) and red band divided by their sum, as follows:

NDVI= (NIR-RED) / (NIR+RED)

where RED and NIR bands represent spectral reflectance measurement in the red band and near infrared band, respectively

Sensors with NIR and Red bands such as the Advanced Very High Resolution Radiometer (AVHRR), Moderate-resolution Imaging Spectro-radiometer (MODIS), and Satellite pour

l'Observation de la Terre (SPOT) are available to generate NDVI images. Recent research uses NDVI to reveal climate variation [*de Beurs and Henebry, 2008; Stige et al., 2006*], vegetation change [*Heumann et al., 2007; Jeyaseelan et al., 2007*], and trend analysis of phenology [*Olsson et al., 2005*].

A number of NDVI products for studying LSP are available to the public. The Global Inventory Modeling and Mapping Studies (GIMMS) group has developed a dataset with more than 25 years of NDVI observations. It has 16-day composites and is based on the records of NOAA AVHRR series sensors [*Tucker et al., 2005*]. VEGETATION 1 and VEGETATION 2 sensors installed on SPOT4 and SPOT5 satellites, which are operated by the VEGETATION Programme, also provide NDVI records for LSP studies [*Beck et al., 2006*]. The Land Processes Distributed Active Archive Center (LP DAAC) provides MODIS NDVI (MOD13) images that are ready to use.

Sources of available NDVI data differ in spatial resolution and temporal coverage. For example, AVHRR NDVI data is extended from 1981 to present; while fewer than years of data are accessible from modern sensors such as MODIS (11 years) and SPOT (13 years) [*Pettorelli et al., 2005*]. Although AVHRR sensors give an invaluable and irreplaceable archive of historical land surface information, they were not designed for vegetation monitoring originally [*Teillet et al., 1997*]. Three factors affect the reliability of the AVHRR NDVI data: 1) the sensors are sensitive to water vapor in the atmosphere, which impacts the calculated NDVI value [*Cihlar et al., 2002*]; 2) The data reduction method, which transfers the local area coverage AVHRR data to AVHRR-NDVI data and changes the spatial resolution from 1 km to 8 km, bears on its quality [*James and Kalluri, 1994*]; 3) the orbital drift of the sensors during their lifetime influences the geometric system and in turn affects the image quality [*Cihlar et al., 2002; Fensholt et al., 2009*].

The wide use of AVHRR NDVI data not only extended the intended applications of historical sensors, but also stimulated the development of modern sensors like MODIS and SPOT that have higher spatial resolution with improved capability of monitoring LSP [*Tarnavsky et al., 2008; Tucker et al., 2005*]. The newer sensors are better equipped with navigation, atmospheric correction and improved radiometric sensitivity systems [*Gobron et al., 2000*]. The availability of modern global satellite sensor data meets the ever-increasing demand of LSP studies [*Justice et al., 2000*].

Several studies have attempted to evaluate the compatibility of AVHRR NDVI with newer datasets such as MODIS and SPOT [*Brown et al., 2006; Ramsey et al., 1995; Fensholt et al., 2009; Swinnen and Veroustraete, 2008; van Leeuwen et al., 2006*]. *Fensholt et al., (2009)* applied linear least squares trend analysis to annual average NDVI of different datasets. Some experiments evaluated the relative and absolute differences of NDVI data within a region or several selected sites over the world [*Brown et al., 2006; Ramsey et al., 1995*]. New vegetation indices were developed as reference index in a comparison carried out by *Kim et al., (2007)* in the Brazilian rain forest. Their expectation was to substitute NDVI by other VIs in cross sensor application.

In this work, I propose that although there are dissimilarities in data construction, phenophases derived from multi-sensors NDVI data follow a linear relationship with one another if compared within the eco-region framework of the Contiguous US. To test this hypothesis I collected NDVI products derived from AVHRR, MODIS, and SPOT sensors, and calculated the Start of Season (SOS) and End of Season (EOS) of each sequence. SOS/EOS values from multi-sensor images were analyzed within the eco-region boundary of Contiguous US. In order to further verify my hypothesis, I collected 1127 sample points randomly over the study area. The

objective of this work was to evaluate the difference and similarity of various NDVI products when used in LSP studies, and provide further understanding of possibility to merge multi-sensor NDVI data for future phenological studies.

2.2 Study Area

For my study area, I selected the Contiguous United States which includes 48 US states, and excludes Alaska, Hawaii, and all off-shore US territories. The study area spans over 8,080,464.3 km^2, with 5.2% of water area [*U. S. Bureau, 2000*]. I selected this region because it provides a wide variety of eco-regions at moderate latitudes and is not affected by known issues in far northern or equatorial areas. It has been shown that AVHRR NDVI performs poorly in high latitude environments [*Beck et al., 2006*], as a result of short growing season, snow cover, and long interval of darkness in winter. Images derived from low latitude areas are strongly affected by cloud cover, which causes inconsistency of SOS/EOS estimations based on NDVI data.

2.3 Data

2.3.1 Satellite Data

The three NDVI time series used in this study are: 1) AVHRR, 2) MODIS, and 3) SPOT VGT NDVI data. The temporal coverage of images ranges from 2000 to 2008. AVHRR-NDVI data was collected by NOAA AVHRR sensors, and developed by the Global Inventory Modeling and Mapping Studies (GIMMS) group. The AVHRR-NDVI product uses bands 1 (0.5 to 0.7 μm) and 2 (0.7 to 1.1 μm). It provides global NDVI data with spatial resolution at 8 km [*Tucker et al., 2003*], a 15-day time step. Images dated from early 2000 were derived from NOAA-14, while

NOAA-16 provides images after November 2000 [*Tucker et al., 2005*]. All images were rescaled to a spatial resolution of 8 km to match AVHRR products.

MODIS NDVI images were derived from MOD43 BRDF Nadir BRDF-Adjusted Reflectance (NBAR) data at 0.05 °(5.6km) spatial resolution. I used a maximum value compositing method to composite the data into a 16-day base from the original 8-day resolution. Both Terra and Aqua instruments were used in the product generation. The Land Processes Distributed Active Archive Center (LP DAAC) selected MODIS bands 1 and 2, which range from 0.62 to 0.67 μm and 0.84 to 0.87 μm for NDVI data calibration.

The VGT-S10 products from SPOT NDVI data were used in this study. Images were taken by the SPOT series sensors with a ten-day interval. The B2 spectral band (0.61 - 0.68 μm) and B3 spectral band (0.78 - 0.89 μm) were chosen as the red and NIR bands respectively. An overview of the available datasets can be found in Table 2. Both MODIS and SPOT data were re-projected to Albers projection to correspond with the AVHRR data.

2.3.2 Eco-regions

The U.S. Environmental Protection Agency (EPA) provides a system of eco-regions of North America at four different levels. The EPA eco-region frameworks were originally derived from Omernik's framework and last updated in 2003[*Omernik, 1995; 2004*]. The Level I division is the coarsest division with 15 classes, while level II has 50 classes. The eco-regions have been further subdivided into 84 categories within the level III division. Level IV is a more detailed division [*Bryce et al., 1999; Omernik et al., 2000*]. In this study, I downloaded the EPA eco-regions of Contiguous U.S. at Level III in shapefile format, and highlighted the boundary of each region in red.

2.3.3 Land Cover Image

Finally, I obtained a land cover image of North America from the National Center for Earth Resources Observation and Science, USGS National Map Seamless server (http://seamless.usgs.gov/index.php), published in Dec 2002. The land cover classes were produced using AVHRR image at 1 km spatial resolution from April 1992 to March 1993. Twenty four land cover categories are displayed in the image. The land cover data was used in the second step of the data comparison, in which 1127 sample points were created randomly and assigned to different land cover classes based on the proportion of their area.

2.4 Methodology

Rather than discuss effects caused by the differences in temporal, spectral and spatial resolutions between multi-sensor datasets, I use a model to estimate SOS/EOS (discussed below) and compare SOS/EOS instead of raw NDVI data. Unlike using NDVI data, the biggest advantage of comparing SOS/EOS is that only two images per year will be compared. The idea is to extract SOS/EOS date for each eco-region and sample point, and then conduct a linear regression analysis for different datasets within the unit of eco-regions or points.

Annual AVHRR, MODIS, and SPOT NDVI images from 2000 to 2008 were downloaded and stacked. There are 24 composites per year for the AVHRR data, and 23 composites per year for MODIS. SPOT images are produced every 10 days; as a result, there are 36 composites per year for SPOT.

Many methods are available to calculate the SOS and EOS dates. It is difficult to select an appropriate method to determine the SOS/EOS of area at large scale. *White et al., (2009)*

explored the difference of ten methods that were used in recent phenological research. They proposed the term Start of Season (SOS), and investigated gaps between field-observed SOS and model estimations. It reveals that the HANTS-FFT and Mid-point $_{pixel}$ methods showed higher overall accuracy of SOS/EOS estimates in North America compared to other models. Therefore, I selected the Mid-point $_{pixel}$ method (with threshold NDVI $_{ratio}$ =50% to determine the annual SOS and EOS. *White et al., (1997)* developed a formula to transform NDVI value (ranges from -1 to 1) to NDVI $_{ratio}$ as,

$$\mathbf{NDVI_{ratio} = (NDVI - NDVI_{min}) / (NDVI_{max} - NDVI_{min})}$$

where NDVI is the original composite NDVI value, NDVI $_{max}$ is the annual maximum NDVI, and NDVI $_{min}$ is the annual minimum NDVI. By using the Mid-point $_{pixel}$ method, SOS is defined as the point in the time when the NDVI $_{ratio}$ annual curve first reaches 0.5, while EOS is defined when the curve drops back passed the 0.5 mark (Figure 3).

In order to remove errors in SOS/EOS images, I filtered out pixels with missing values or estimates beyond the range from 0 to 360. Because AVHRR data has the coarsest spatial resolution, SOS/EOS results calculated by MODIS and SPOT datasets are aggregated to 8 km. This provides a common spatial resolution and enables the comparison of sample points to be conducted using standardized images. To filter noisy pixels and account for location inaccuracies, I applied a median filter with a window of 5 by 5 pixels. The value of each cell was replaced by the median value of its neighboring entries. The median filter reassigned the isolated pixels, and presents a coherent image pattern [*Beltran and Belmonte, 2001*].

There are millions of pixels that carrying phenological information. As a result, it's difficult to compare every pixel by datasets. In addition, the geometric accuracy of some of the images is low. Two methods were applied to simplify the comparison and prevent errors due to geometric

issues: 1) by eco-region framework and, 2) by sample points. The data were first compared within an eco-region framework. I calculated the zonal statistics for each eco-region. The annual SOS/EOS for each eco-region was depicted by the average SOS/EOS of every valid pixel within that area. Eco-regions with inconsistent or unstable values of annual average SOS/EOS through 9 years were not used in comparison. Most of these removed eco-regions were small islands next to the western and southern coast of Contiguous US. SOS/EOS value were plotted pair-wisely and fitted with regression lines. R-square indicates the correlation between datasets.

The second step was based on land cover. I computed the area of each land cover within the extent of the Contiguous US. Consistent to the land cover proportion, sample points were divided into different categories. Several detailed land cover classes were merged into roughly 6 categories. As a result, I allocated 9 points to urban, 312 points to Cropland, 312 points to Scrubland and Grassland, 378 points to Forest. The remaining 22 points represent other land cover types. I extracted pixel values of SOS/EOS estimation to sample points by bilinear interpolation; the value of each sample point is the weighted average of the cell and its surrounding pixels.

2.5 Results

I evaluated the percentage of valid pixels in each image (Table 3), and found that: 1) the AVHRR dataset has the highest rate of applicable pixels. The average percentages of valid estimations for SOS and EOS were 95% and 97%, respectively. The difference of sensors' sensitivity to cloud covers in low latitude area influence the accuracy of SOS/EOS evaluation; 2) the MODIS dataset has a lower validity than AVHRR dataset. The proportion of valid MODIS-SOS estimations dropped to 67.7% in 2001. However, the MODIS-EOS estimation shows a

higher percentage of valid estimates. 3) The overall rates of SPOT estimation accuracy are between 53% and 72%. With an average percentage of valid estimation about 65%, SPOT-NDVI does not function well in monitoring vegetation growth in the southern part of the study area (Table 3) due to the large amount of missing data in the original images. As a result, the SPOT dataset has relatively poor accuracy of growing season estimation for those regions.

2.5.1 Eco-region Comparison of SOS/EOS Estimation

In the comparison of eco-regions, some area produced invalid estimate of annual average SOS/EOS (e.g. eco-region with less than 5 years' records of SOS/EOS estimation is considered to be invalid eco-region). Therefore, eco-regions with an insufficient number of valid pixels of SOS/EOS estimation were not used in linear regression. Table 4 indicates that the largest number of eco-regions that contains phenological information was derived from the AVHRR dataset, due to the high percentage of valid SOS/EOS evaluation. The MODIS dataset produced lower numbers of comparable eco-regions than AVHRR on average. Less than 40% of all eco-regions contained enough SOS/EOS estimations from SPOT. Most eco-regions provided consistent SOS/EOS estimations. Figure 4.1 shows the SOS estimation based on AVHRR, MODIS, and SPOT within the Driftless area as an example. Both MODIS and AVHRR profiles provide smooth and stable patterns over 9 years. The curve of SPOT dataset is more fluctuated than other datasets (ranges from 113 to144), which indicates it has larger variation. The EOS estimation has clearer inconsistency among the 9 years period. In the Driftless Area, MODIS estimates a later arrival of SOS and EOS than other datasets. In 2001 and 2004, three datasets showed great disagreement in SOS/EOS assessment.

The statistics of the SOS/EOS estimation for each sensor are shown in box plots (Figure 5). The box plots and distribution patterns indicate that, on average, SPOT-NDVI estimates later SOS value than do the other datasets. Figure 5.2 reflects a slightly later arrival of EOS date computed by MODIS dataset over the study area. EOS box plots show larger variation among their estimations.

I evaluated the dataset differences between AVHRR, MODIS, and SPOT by eco-regions (Figure 6). The root mean square error (RMSE) between datasets was mostly in the range of 14 to 27 days. The EOS comparison between MODIS and SPOT resulted in the greatest RMSE (26.5 days), and the combination of AVHRR-SOS /SPOT-SOS reported the lowest RMSE (10.5). For the SOS estimation, AVHRR/SPOT was better correlated, with R-square close to 0.7 and RMSE of 10.5. The distribution of the points showed a compact pattern and followed a straight line. The correlation between MODIS and SPOT is slightly stronger than AVHRR and MODIS. EOS estimation plotted a broader variety of point distributions than SOS estimation. Most of the points were narrowed to the extent within 200 to 350. Likewise, AVHRR/SPOT has the lowest RMSE and highest R-Square, compared with other combinations. The AVHRR /MODIS plot was more complicated. The points were diversely spread along the ordinary least squares (OLS) line, between 100 and 340. The majority of the points were aggregated from 250 to 320. MODIS-EOS of 2001 was much higher than other years (symbolized by red squares), which were present in a vertical pattern on the EOS-AVHRR/MODIS graph, while data captured in 2001 are showing a horizontal pattern on EOS MODIS/SPOT graph.

2.5.2 Sample Point Comparison of SOS/EOS Estimation

To present the R-Square values between multiple datasets in different land cover classes, I fitted x (explanatory variable) and y (dependent variable) to three datasets, and plotted those dots by land cover (Cropland, Scrubland & Grassland, and Forest). With 9 years of data, more than 2000 points were plotted for those three classes. Table 5 summarizes the correlation of the SOS and EOS values computed from different datasets by land cover. The variation of R-Square value in this table shows that SOS/EOS derived from different datasets are not evenly correlated, due to the characteristics of sensors and methods used to process data (discussed above). Except the group of AVHRR and SPOT datasets in urban area, each datasets combination shows higher correlation in SOS estimation than that in EOS, largely due to the higher accuracy of SOS estimation than EOS in general [*Delbart et al., 2005*].

Correlation of data sensor combinations was strongly affected by land cover. On average, urban areas illustrated high correlations of datasets both in SOS and EOS images. Given the small sample size that only 9 points were generated in such category, comparison carried out within urban area could not provide persuasive evidence for linear relationship between datasets. The highest R-Square values occur in AVHRR/SPOT comparison regardless of land cover, which corresponds with the eco-region comparison. High R-Square reflects a strong association between AVHRR and SPOT datasets over Contiguous United States. In the area of Cropland, Scrubland & Grassland, and Forest, the AVHRR /MODIS sensor combination has higher correlation than MODIS /SPOT for SOS estimation, but lower for EOS. Larger intercepts of EOS regression lines (Table 6) than that of SOS indicate that EOS estimation further exaggerates the difference of phenologial estimation between datasets.

2.6 Discussion

Fensholt et al., (2009) compared multi-sensors NDVI data in Senegal and created equations to standardize GIMMS AVHRR, MODIS, and SPOT VGT NDVI to annual average NDVI based on ground observation. I transformed their equations to pair-wise sensors comparison base. *van Leeuwen et al., (2006)* developed NDVI conversion equation between AVHRR and MODIS datasets by using $AVHRR_{14,}$ $AVHRR_{16,}$ and MODIS NDVI image within the extent of Arizona. To compare their work with my phenological analysis, I extracted slopes of NDVI equations from their studies and my SOS/EOS regression lines (Table 7). *van Leeuwen et al., (2006)* concluded a close similarity between AVHRR and MODIS dataset with a slope of 0.98. The highest correlation between AVHRR and MODIS SOS/EOS estimation is found in cropland area. Similar to the findings of Fensholt et al., (2009), my analysis found a higher resemblance between AVHRR and SPOT data than other dataset combinations. Phenological evaluation provides a maximum slope of 0.808 between EOS images of AVHRR and SPOT in cropland area. However, a better agreement was observed directly by using NDVI data (slope=0.930). Overall, slope of the regression suggests that similarities between SOS/EOS derived from multiple datasets agree with those results from NDVI dataset. However, some areas have relatively low agreement between two datasets using SOS/EOS images (e.g., a slope of 0.52 in the forest area). Although AVHRR and SPOT datasets have the greatest agreement if compared either in form of SOS/EOS outputs or raw NDVI data, one should be careful to choose study area when using SPOT data to interpolate AVHRR for phenological study.

By using an eco-region framework and random points, I was able to get a sample of SOS/EOS records from different NDVI products. It revealed that AVHRR-NDVI is strongly correlated with SPOT NDVI data. However, according to Table 3, the SPOT data results the lowest percentage of valid pixels after data refinement, which means low ratio of applicable

pixels was used in SOS/EOS modeling. A possible reason could be the diversity of sensor's sensitivity to water vapor in area with high percentage of cloud cover [*van Leeuwen et al., 2006*]; in this case, the southern part of Contiguous U.S. As a result, lots of eco-regions could not be used in the data comparison due to insufficient data. Further research is suggested to verify the reasons for the low percentage of valid pixels in NDVI images. MODIS data in 2001 and 2002 appear messier than in subsequent years. In this study I used the MODIS BRDF dataset. This is based on Terra data before 2002. With the launch of Aqua in 2002, the dataset utilizes both sensors resulting in a much more stable product. It appears that EOS estimation in 2001 is flawed (Table 3 & 4).

2.7 Conclusion

With the launch of multiple sensors, NDVI data derived from various sources can be used to provide biophysical measurements for phenological studies. I found that the NDVI products of AVHRR, MODIS, and SPOT datasets follow linear and positive relationships, which were reflected by the comparison of estimated SOS/EOS dates. If used in phenological study, it is possible to use multi-sensor NDVI products for SOS/EOS modeling without applying the multi-sensor NDVI conversion equations. However, long time consistency and continuity of future NDVI products should be confirmed. Otherwise, additional efforts should be made to guarantee the image quality of NDVI data derived from multiple sensors.

Future research should include: 1) field observations of SOS/EOS collected by phenological network sites to verify the results calculated my work, 2) data transformed by conversion

equation to further support the hypothesis that multi-sensor NDVI data can be used in phenological modeling without concern for data divergence.

Benefits of this work include: 1) enables the merging of AVHRR-NDVI, MODIS-NDVI, and SPOT-NDVI data for phenological study without concern for differences in spectral, spatial, and temporal resolutions, 2) fill the void of the knowledge on how to apply alternative method in multi-sensor NDVI data comparison for phenological research, 3) further prove the statement that NDVI data from alternative sensors can substitute for gaps in a dataset for phenological modeling, 4) recommend future research of multi-sensor NDVI data analysis for phenology.

References List

Beck, P., C. Atzberger, K. Høgda, B. Johansen, and A. Skidmore (2006), Improved monitoring of vegetation dynamics at very high latitudes: a new method using MODIS NDVI, *Remote Sensing of Environment*, *100*(3), 321-334.

Beltran, C. M., and A. C. Belmonte (2001), Irrigated crop area estimation using Landsat TM imagery in La Mancha, Spain, *Photogrammetric Engineering and Remote Sensing*, *67*(10), 1177-1184.

Brown, M., J. Pinzón, K. Didan, J. Morisette, and C. Tucker (2006), Evaluation of the consistency of long-term NDVI time series derived from AVHRR, SPOT-vegetation, SeaWiFS, MODIS, and Landsat ETM+ sensors, *Geoscience and Remote Sensing, IEEE Transactions on*, *44*(7), 1787-1793.

Bryce, S., J. Omernik, and D. Larsen (1999), Environmental Review: Ecoregions: A Geographic Framework to Guide Risk Characterization and Ecosystem Management, *Environmental Practice*, *1*(03), 141-155.

U. S. Bureau, (2000), Geographic Identifiers.

Cihlar, J., I. Tcherednichenko, R. Latifovic, Z. Li, and J. Chen (2002), Impact of variable atmospheric water vapor content on AVHRR data corrections over land, *Geoscience and Remote Sensing, IEEE Transactions on*, *39*(1), 173-180.

de Beurs, K. M. and G. M. Henebry (2008). "War, drought, and phenology: changes in the land surface phenology of Afghanistan since 1982." Journal of Land Use Science 3(2): 95-111.

Delbart, N., L. Kergoat, T. Le Toan, J. Lhermitte, and G. Picard (2005), Determination of phenological dates in boreal regions using normalized difference water index, *Remote Sensing of Environment*, *97*(1), 26-38.

Ramsey, R. Douglas, A. Falconer, and J. Jensen (1995), The relationship between NOAA-AVHRR NDVI and ecoregions in Utah, *Remote Sensing of Environment*, *53*(3), 188-198.

Fensholt, R., K. Rasmussen, T. Nielsen, and C. Mbow (2009), Evaluation of earth observation based long term vegetation trends--Intercomparing NDVI time series trend analysis consistency of Sahel from AVHRR GIMMS, Terra MODIS and SPOT VGT data, *Remote Sensing of Environment*, *113*(9), 1886-1898.

Gobron, N., B. Pinty, M. Verstraete, and J. Widlowski (2000), Development of spectral indices optimized for the VEGETATION Instrument.

Heumann, B., J. Seaquist, L. Eklundh, and P. Jönsson (2007), AVHRR derived phenological change in the Sahel and Soudan, Africa, 1982-2005, *Remote Sensing of Environment*, *108*(4), 385-392.

James, M., and S. N. V. Kalluri (1994), The Pathfinder AVHRR land data set: an improved coarse resolution data set for terrestrial monitoring, *International Journal of Remote Sensing*, *15*(17), 3347-3363.

Jeyaseelan, A., P. Roy, and S. Young (2007), Persistent changes in NDVI between 1982 and 2003 over India using AVHRR GIMMS (Global Inventory Modeling and Mapping Studies) data, *International Journal of Remote Sensing*, *28*(21), 4927-4946.

Justice, C., A. Belward, J. Morisette, P. Lewis, J. Privette, and F. Baret (2000), Developments in the'validation'of satellite sensor products for the study of the land surface, *International Journal of Remote Sensing*, *21*(17), 3383-3390.

Kang, S., S. Running, J. Lim, M. Zhao, C. Park, and R. Loehman (2003), A regional phenology model for detecting onset of greenness in temperate mixed forests, Korea: an application of MODIS leaf area index, *Remote Sensing of Environment*, *86*(2), 232-242.

Kim, Y., A. R. Huete, Z. Jiang, and T. Miura (2007), Multisensor reflectance and vegetation index comparisons of Amazon tropical forest phenology with hyperspectral Hyperion data, *Remote Sensing and Modeling of Ecosystems for Sustainability IV*, *6679*(667906-1).

Morisette, J., A. Richardson, A. Knapp, J. Fisher, E. Graham, J. Abatzoglou, B. Wilson, D. Breshears, G. Henebry, and J. Hanes (2008), Tracking the rhythm of the seasons in the face of global change: phenological research in the 21st century.

Moulin, S., L. Kergoat, N. Viovy, and G. Dedieu (1997), Global-scale assessment of vegetation phenology using NOAA/AVHRR satellite measurements, *Journal of Climate*, *10*(6), 1154-1170.

Myneni, R., S. Hoffman, Y. Knyazikhin, J. Privette, J. Glassy, Y. Tian, Y. Wang, X. Song, Y. Zhang, and G. Smith (2002), Global products of vegetation leaf area and fraction absorbed PAR from year one of MODIS data, *Remote Sensing of Environment*, *83*(1-2), 214-231.

Olsson, L., L. Eklundh, and J. Ardö (2005), A recent greening of the Sahel--trends, patterns and potential causes, *Journal of Arid Environments*, *63*(3), 556-566.

Omernik, J. (1995), Ecoregions: a spatial framework for environmental management, *Biological assessment and criteria: tools for water resource planning and decision making*, 49–62.

Omernik, J. (2004), Perspectives on the nature and definition of ecological regions, *Environmental Management*, *34*, 27-38.

Omernik, J., S. Chapman, R. Lillie, and R. Dumke (2000), Ecoregions of Wisconsin, *Transactions of the Wisconsin Academy of Sciences, Arts, and Letters*, *88*(2000), 77-103.

Pettorelli, N., J. Vik, A. Mysterud, J. Gaillard, C. Tucker, and N. Stenseth (2005), Using the satellite-derived NDVI to assess ecological responses to environmental change, *Trends in Ecology & Evolution*, *20*(9), 503-510.

Reed, B., J. Brown, D. VanderZee, T. Loveland, J. Merchant, and D. Ohlen (1994), Measuring phenological variability from satellite imagery, *Journal of Vegetation Science*, *5*(5), 703-714.

Stige, L. C., J. Stave, K. S. Chan, L. Ciannelli, N. Pettorelli, M. Glantz, H. R. Herren, and N. C. Stenseth (2006), The effect of climate variation on agro-pastoral production in Africa, *Proceedings of the National Academy of Sciences of the United States of America*, *103*(9), 3049.

Swinnen, E., and F. Veroustraete (2008), Extending the SPOT-VEGETATION NDVI time series (1998–2006) back in time with NOAA-AVHRR data (1985–1998) for southern Africa, *Geoscience and Remote Sensing, IEEE Transactions on*, *46*(2), 558-572.

Tarnavsky, E., S. Garrigues, and M. Brown (2008), Multiscale geostatistical analysis of AVHRR, SPOT-VGT, and MODIS global NDVI products, *Remote Sensing of Environment*, *112*(2), 535-549.

Teillet, P., K. Staenz, and D. William (1997), Effects of spectral, spatial, and radiometric characteristics on remote sensing vegetation indices of forested regions, *Remote Sensing of Environment*, *61*(1), 139-149.

Tucker, C. (1979), Red and photographic infrared linear combinations for monitoring vegetation, *Remote Sensing of Environment*, *8*(2), 127-150.

Tucker, C., R. Mahoney, N. El-Saleous, S. Los, M. Brown, M. Paris, D. Grant, and A. Morahan (2003), The global inventory mapping and monitoring study 1981–1999 AVHRR 8-km data set, *Int. J. Remote Sens.*

Tucker, C., J. Pinzón, M. Brown, D. Slayback, E. Pak, R. Mahoney, E. Vermote, and N. El Saleous (2005), An extended AVHRR 8-km NDVI dataset compatible with MODIS and SPOT vegetation NDVI data, *International Journal of Remote Sensing*, *26*(20), 4485-4498.

van Leeuwen, W., B. Orr, S. Marsh, and S. Herrmann (2006), Multi-sensor NDVI data continuity: Uncertainties and implications for vegetation monitoring applications, *Remote sensing of environment*, *100*(1), 67-81.

White, M., P. Thornton, and S. Running (1997), A continental phenology model for monitoring vegetation responses to interannual climatic variability, *Global Biogeochemical Cycles*, *11*(2), 217-234.

White, M., K. de Beurs, K. Didan, D. Inouye, A. Richardson, O. Jensen, J. O'Keefe, G. Zhang, R. Nemani, and W. van Leeuwen (2009), Intercomparison, interpretation, and assessment of spring phenology in North America estimated from remote sensing for 1982–2006, *Global Change Biology*, *15*(10), 2335-2359.

Zhang, X., M. Friedl, C. Schaaf, A. Strahler, J. Hodges, F. Gao, B. Reed, and A. Huete (2003), Monitoring vegetation phenology using MODIS, *Remote Sensing of Environment, 84*(3), 471-475.

Tables and Figures

Table 2 Attributes of NDVI Data

Sensor	AVHRR	SPOT VGT	MODIS
Satellites	NOAA-7, 9, 11, 14, and 16	SPOT4 and SPOT 5	Terra and Aqua
Launch Date	23 Jun 1981 (NOAA-7)	24 Mar 1998 (SPOT4)	18 Dec 1999 (Terra)
Data Source	GIMMS NDVI	VEGETATION Programme	LP DAAC
Red/NIR Band (μm)	(0.5-0.7)/(0.7-1.1)	(0.61-0.68)/(0.78-0.89)	(0.62-0.67)/(0.84-0.87)
Spatial Resolution(km)	8	1	5.6
Temporal Resolution (days)	15	10	16
Coverage	Global	*North America	Global

*Coverage of available SPOT NDVI products from Vegetation Programme is North America (not global); they are further divided into northern, central, and southern North America

Table 3 Percentage of Valid SOS/EOS Estimation:
Pixels with SOS/EOS value less than or equals to 0 were deleted. SOS/EOS values generated from AVHRR or MODIS datasets that were larger than 360 were considered as invalid. SPOT-EOS dates later than day 355 were removed as well.

Percentage of Valid Pixel= the Number of Valid Pixels divided by the Total Number of Pixels within Study Area

Valid Pixel		2000	2001	2002	2003	2004	2005	2006	2007	2008
AVHRR	SOS	96.0%	96.9%	92.3%	95.8%	97.7%	96.2%	89.5%	95.0%	96.3%
	EOS	97.9%	98.9%	97.4%	98.7%	94.1%	96.9%	92.6%	97.4%	97.1%
MODIS	SOS	87.5%	67.9%	88.1%	88.0%	94.3%	93.2%	86.5%	93.0%	95.4%
	EOS	88.4%	99.6%	84.8%	90.4%	82.2%	91.2%	88.1%	90.5%	93.4%
SPOT	SOS	71.2%	67.2%	56.1%	67.0%	53.3%	73.6%	60.5%	71.5%	68.6%
	EOS	71.2%	65.9%	57.4%	65.6%	51.6%	71.5%	60.9%	71.9%	68.5%

Table 4 Percentage of Valid Eco-regions:
Eco-regions with SOS/EOS value were removed if they meet these following criteria: 1) Standard Deviation (STD) of 9-year records beyond the range: Mean of 9-year records' STDs +/- 2* STD of 9-year records' STDs; 2) Eco-region that has less than 5-year's valid records. Percentage of Valid Eco-region= the Number of Valid Eco-regions divided by the Total Number of Eco-regions within Study Area (84 Eco-region in Contiguous U.S.)

Valid Eco-region		2000	2001	2002	2003	2004	2005	2006	2007	2008
AVHRR	SOS	95.2%	95.2%	91.7%	95.2%	95.2%	94.0%	91.7%	94.0%	95.2%
	EOS	94.0%	94.0%	94.0%	94.0%	94.0%	94.0%	94.0%	94.0%	94.0%
MODIS	SOS	89.3%	60.7%	86.9%	86.9%	89.3%	89.3%	90.5%	89.3%	90.5%
	EOS	90.5%	95.2%	94.0%	85.7%	84.5%	95.2%	92.9%	91.7%	94.0%
SPOT	SOS	70.2%	66.7%	53.6%	66.7%	53.6%	71.4%	60.7%	69.0%	70.2%
	EOS	66.7%	63.1%	58.3%	60.7%	50.0%	71.4%	63.1%	70.2%	71.4%

Table 5 Results of Datasets Comparison by Land Cover:
R-square values of regression analysis are provided by land cover type. The sample size is the number of random sample points by land cover category.

R-Square	SOS			EOS			Sample Size
	AVHRR-MODIS	AVHRR-SPOT	MODIS-SPOT	AVHRR-MODIS	AVHRR-SPOT	MODIS-SPOT	
Urban	0.670	0.584	0.503	0.396	0.803	0.524	9
Cropland	0.608	0.667	0.567	0.272	0.666	0.340	312
Scrubland/Grassland	0.497	0.689	0.413	0.406	0.679	0.416	406
Forest	0.551	0.640	0.411	0.278	0.517	0.289	378

Table 6 Intercepts of Linear Regression Line

Intercept of Linear Regression Line		AVHRR-MODIS	AVHRR-SPOT	MODIS-SPOT
SOS	Eco-region	46.7	25.4	22.6
	Cropland	30.4	20.2	17.8
	Scrubland/Grassland	36.7	18.8	16.3
	Forest	33.4	25.9	29.4
EOS	Eco-region	90.9	86.0	85.1
	Cropland	140.2	49.3	75.4
	Scrubland/Grassland	86.6	51.5	70.2
	Forest	162.8	104.5	101.1

Table 7 Slope of Linear Regression Line

Slope of Linear Regression Line		AVHRR-MODIS	AVHRR-SPOT	MODIS-SPOT
Fensholt et al., (2009)'s Comparison		0.777	0.930	1.198
van Leeuwen et al., (2006)'s Comparison ($AVHRR_{14}/AVHRR_{16}$)		0.975		
		0.973		
SOS	**Eco-region**	0.639	0.687	0.572
	Cropland	0.804	0.715	0.639
	Scrubland/Grassland	0.651	0.724	0.607
	Forest	0.751	0.651	0.520
EOS	**Eco-region**	0.609	0.711	0.761
	Cropland	0.419	0.808	0.718
	Scrubland/Grassland	0.489	0.727	0.741
	Forest	0.397	0.650	0.645

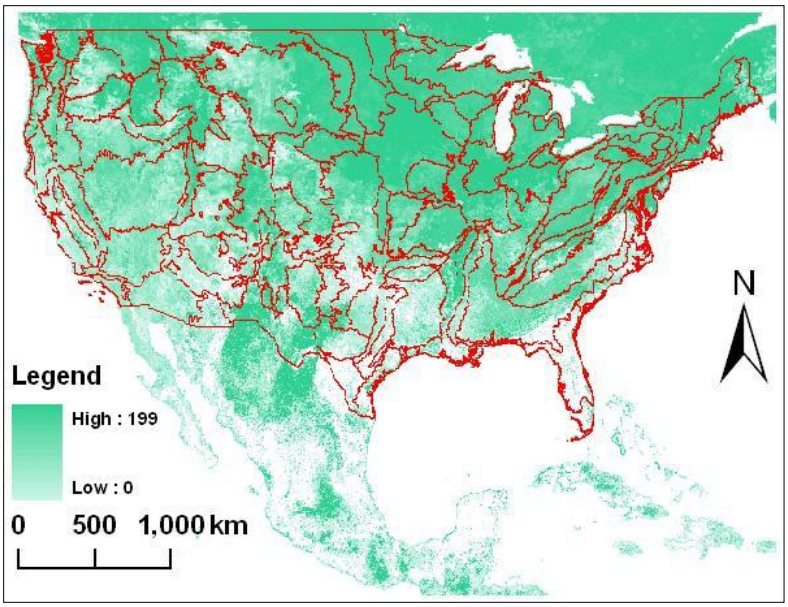

Figure 2 Overview of EPA Eco-region Frameworks
SOS image overlaid with the EPA Level III Eco-region boundary with the extent of Contiguous United States.

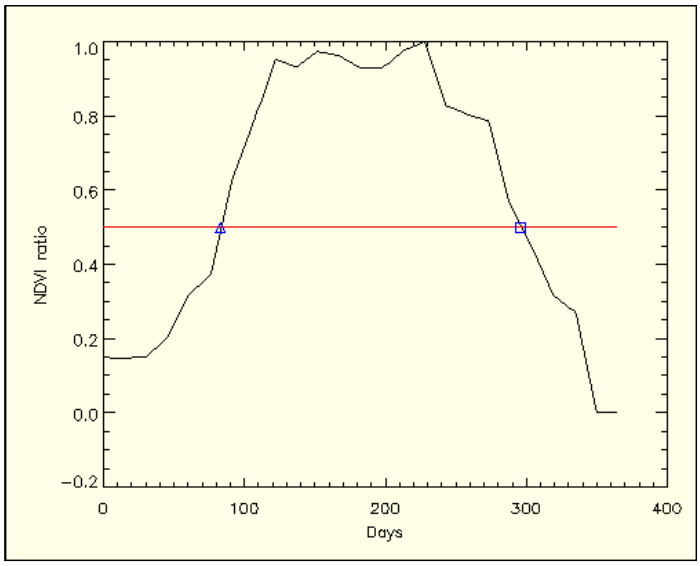

Figure 3 Overview of NDVI Annual Curve

The curve shows NDVI $_{ratio}$ of an entire year (sourced from AVHRR-NDVI in 2006, 15 days' composite). When the Mid-point $_{pixel}$ (NDVI $_{ratio}$= 0.5) applied to this curve, SOS and EOS are determined as the 83rd and 296th day of the year, respectively.

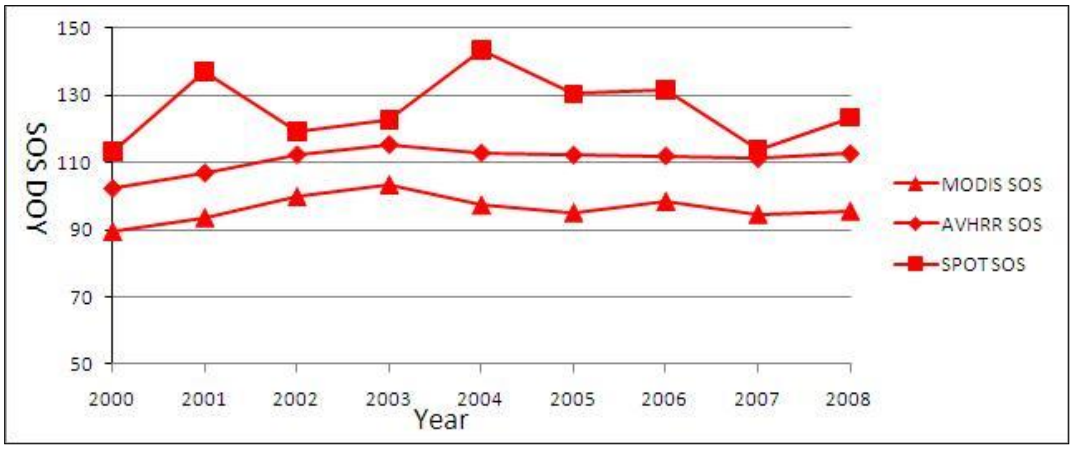

Figure 4.1

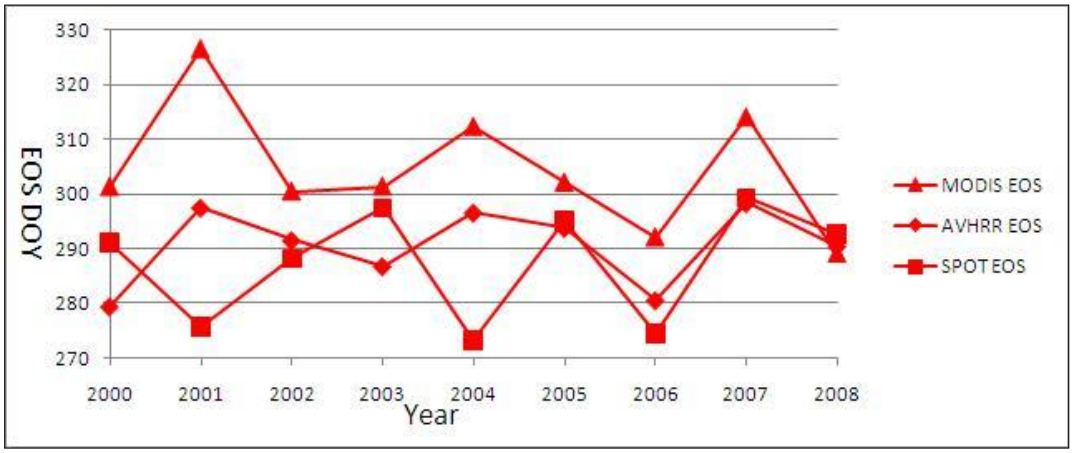

Figure 4.2

Figure 4 Overview of SOS/EOS Estimations in Driftless Area
SOS/EOS profiles for the Driftless area (Eco-region ID: 52), from 2000 to 2008. Date estimation based on AVHRR, MODIS, and SPOT datasets are plotted. All points represent the annual average SOS/EOS date of the area.

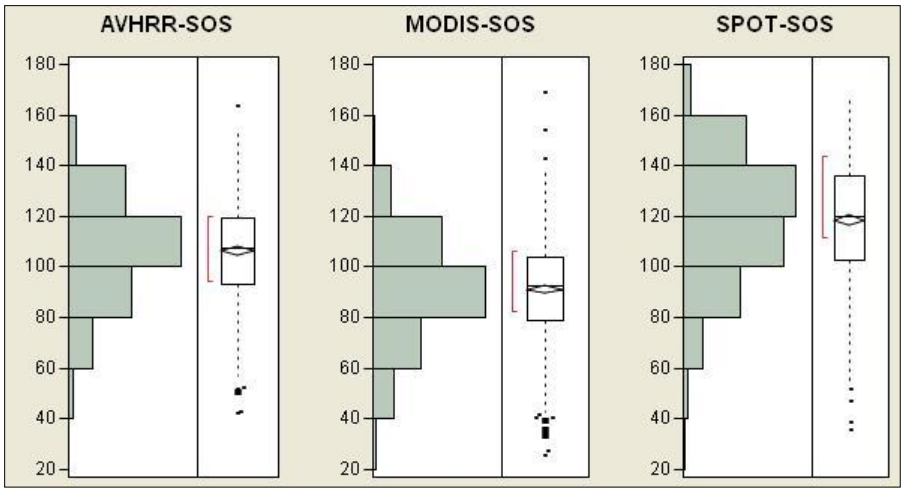

Figure 5.1

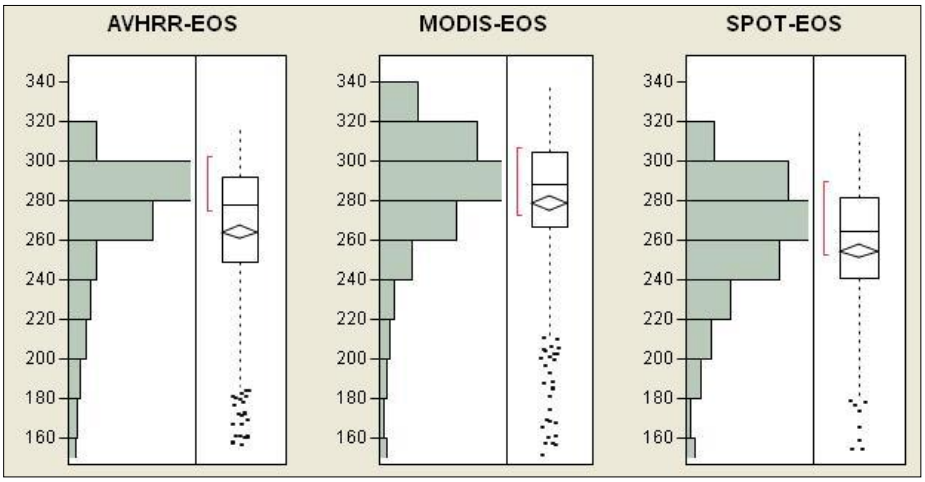

Figure 5.2

Figure 5 Box-plot of SOS/EOS Estimations by Different Datasets

Figure 5.1 plots 532 eco-regions of year; estimation based on SPOT data has the highest mean value. 529 eco-regions of year are plotted on Figure 5.2 MODIS data evaluates a later arrival of EOS in general, with an average of 278.9.

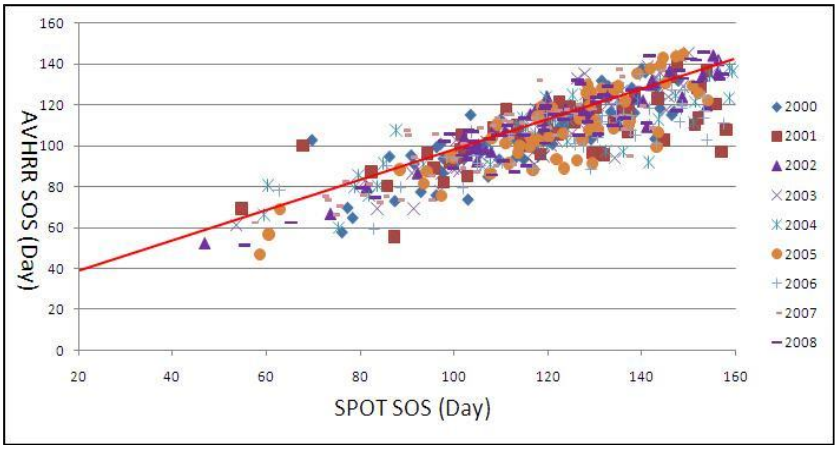

Figure 6.1

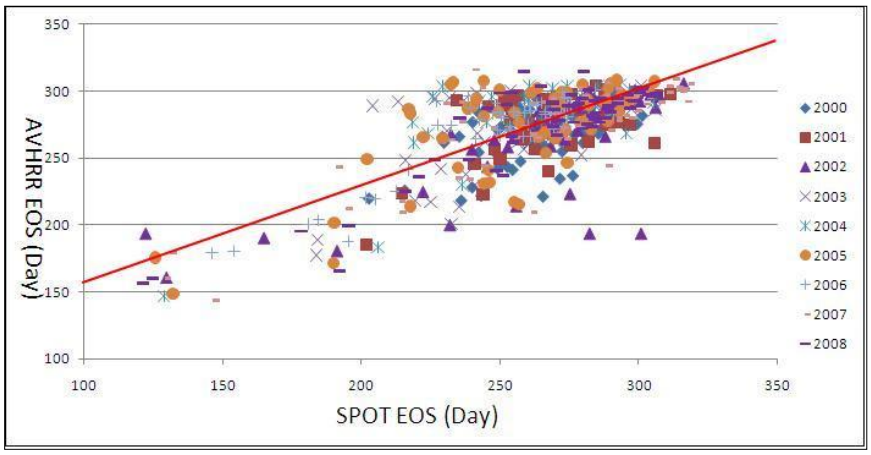

Figure 6.2

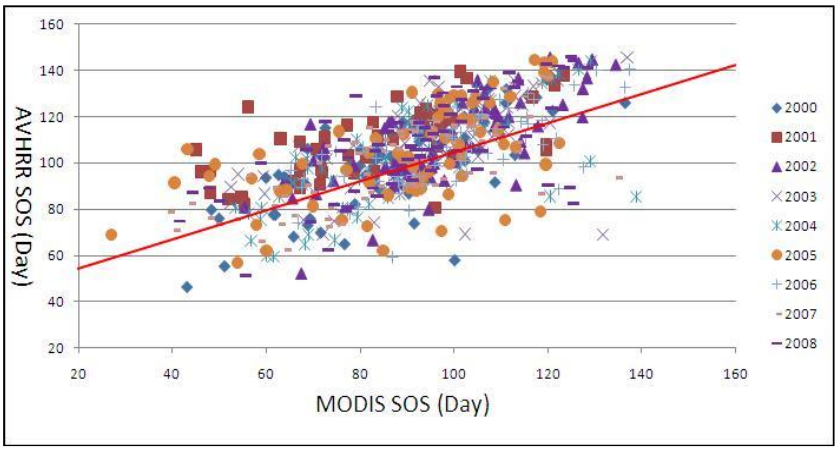

Figure 6.3

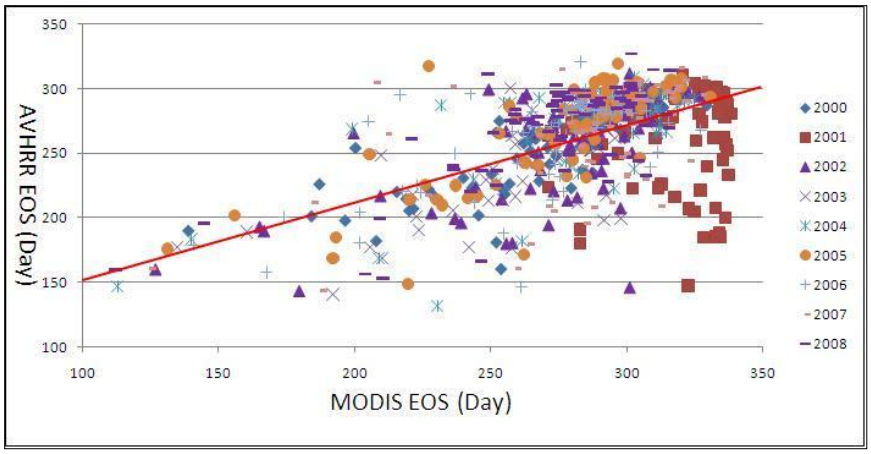

Figure 6.4

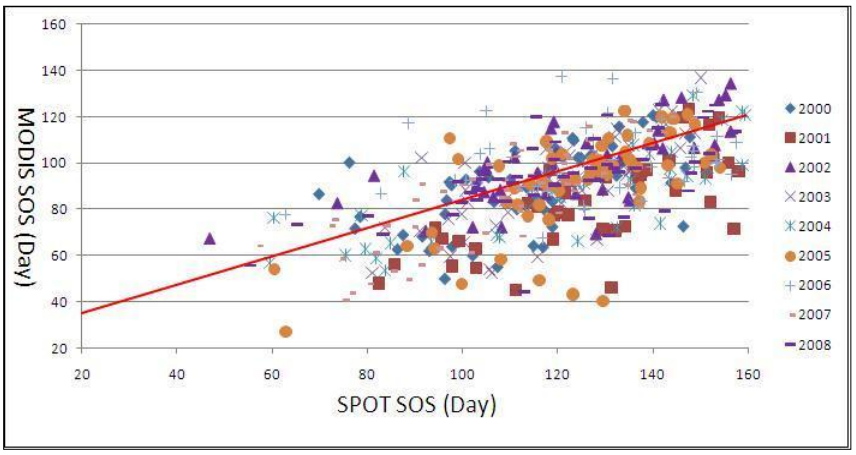

Figure 6.5

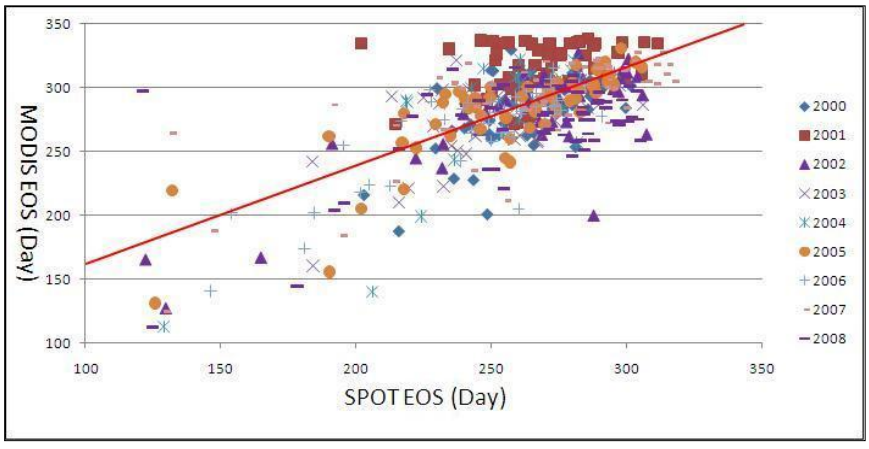

Figure 6.6

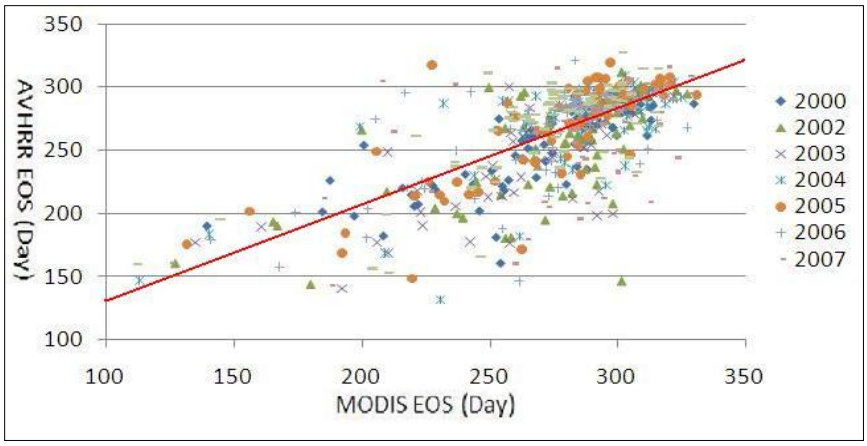

Figure 6.7

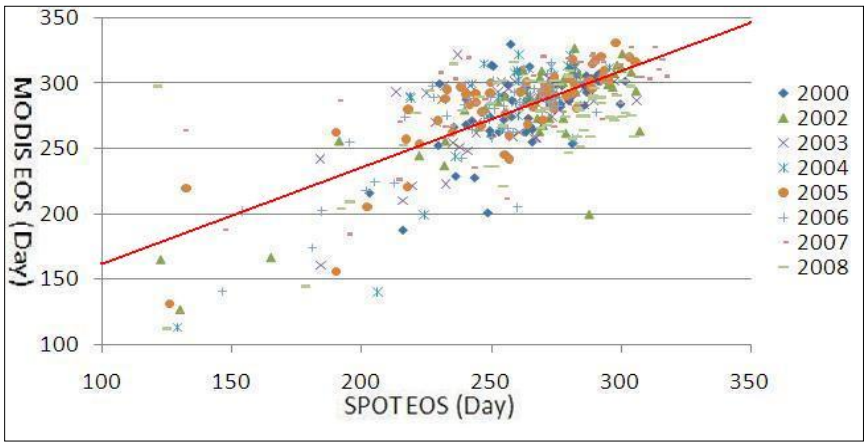

Figure 6.8

Figure 6 Linear Regression of Multi-sensor SOS/EOS Estimations Comparisons

Figure 6.1 Comparison of AVHRR-SOS vs. SPOT-SOS
OLS: AVHRR-SOS = 25.355 + 0.687*SPOT-SOS
R^2 =0.693, RMSE=10.522 (P<0.001), Total Points: 488

Figure 6.2 Comparison of AVHRR-EOS vs. SPOT-EOS
OLS: AVHRR-EOS = 85.980 + 0.711*SPOT-EOS
R^2 =0.585, RMSE= 20.472 (P<0.001), Total Points: 483

Figure 6.3 Comparison of AVHRR-SOS vs. MODIS-SOS
OLS: AVHRR-SOS = 46.739 + 0.639*MODIS-SOS
R^2 =0.438, RMSE=14.213 (P<0.001), Total Points: 648/756

Figure 6.4 Comparison of AVHRR-EOS vs. MODIS-EOS
OLS: AVHRR-EOS = 90.901 + 0.609*MODIS-EOS
R^2 =0.356, RMSE= 30.676 (P<0.001), Total Points: 659

Figure 6.5 Comparison of MODIS-SOS vs. SPOT-SOS
OLS: MODIS-SOS = 22.576+ 0.572*SPOT-SOS
R2 =0.449, RMSE=14.240 (P<0.001), Total Points: 476

Figure 6.6 Comparison of MODIS-EOS vs. SPOT-EOS
OLS: MODIS-EOS = 85.050 + 0.7610*SPOT-EOS
R2 =0.489, RMSE= 26.516 (P<0.001), Total Points: 464

Figure 6.7 Comparison of AVHRR-EOS vs. MODIS-EOS (without MODIS-EOS 2001)
OLS: AVHRR EOS = 61.226 + 0.728*MODIS EOS
R^2 =0.476, RMSE= 27.823 (P<0.001), Total Points: 580

Figure 6.8 Comparison of MODIS-SOS vs. SPOT-SOS (without MODIS-EOS 2001)
OLS: MODIS-EOS = 81.486 + 0.761*SPOT-EOS
R^2 =0.535, RMSE=25.078 (P<0.001), Total Points: 411